nature climate change

SUPPLEMENTARY INFORMATION
https://doi.org/10.1038/s41558-018-0386-4

In the format provided by the authors and unedited.

Global patterns and dynamics of climate–groundwater interactions

M. O. Cuthbert[1,2,3*], T. Gleeson[4,5], N. Moosdorf[6], K. M. Befus[7], A. Schneider[8], J. Hartmann[9] and B. Lehner[10]

[1]School of Earth and Ocean Sciences, Cardiff University, Cardiff, UK. [2]Water Research Institute, Cardiff University, Cardiff, UK. [3]Connected Waters Initiative Research Centre, UNSW Sydney, Sydney, New South Wales, Australia. [4]Department of Civil Engineering, University of Victoria, Victoria, British Colombia, Canada. [5]School of Earth and Ocean Sciences, University of Victoria, Victoria, British Colombia, Canada. [6]Leibniz Centre for Tropical Marine Research (ZMT), Bremen, Germany. [7]Department of Civil and Architectural Engineering, University of Wyoming, Laramie, WY, USA. [8]Sorbonne Université, Milieux environnementaux, transferts et interactions dans les hydrosystèmes et les sols, METIS, Paris, France. [9]Institute for Geology, Center for Earth System Research and Sustainability (CEN), Universität Hamburg, Hamburg, Germany. [10]Department of Geography, McGill University, Montreal, Quebec, Canada. *e-mail: cuthbertm2@cardiff.ac.uk

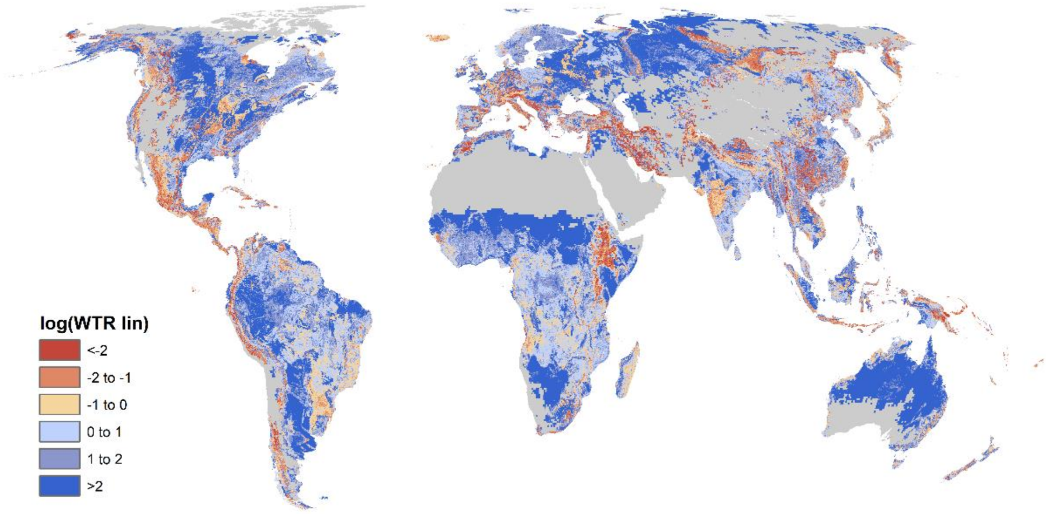

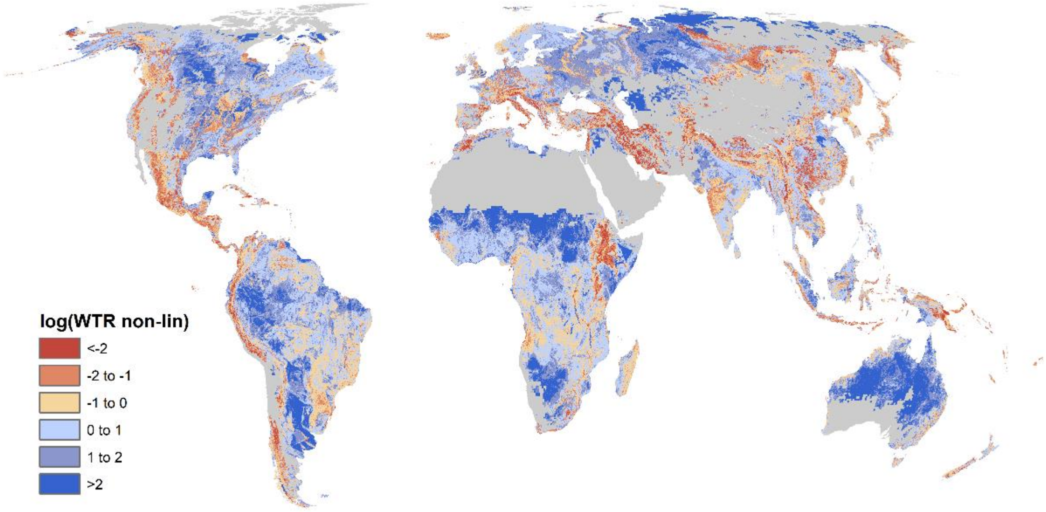

Figure S1 Comparison of global maps of water table ratio (*WTR*) using the previously published[1,2] (WTR lin, Equation 9 in the main text) and new (WTR non-lin, Equation 8) formulation derived for this paper. The new formulation indicates a broad consistency in the regional distribution when compared to the previous linearized formulation, i.e. higher *WTR*s are associated with high humidity, subdued topography and/or low permeability with lower *WTR*s more common in drier climates or more mountainous topography. The frequency distribution comparison (Figure S2) shows that the new formulation has a narrower and more symmetric distribution with a median closer to zero than the linearized form. This is indicative of its better physical representation such that the extent of higher *WTR*s is limited by the feedback between higher water table elevation and concomitant increases in transmissivity inherent in the non-linear Boussinesq equation (Equation 1).

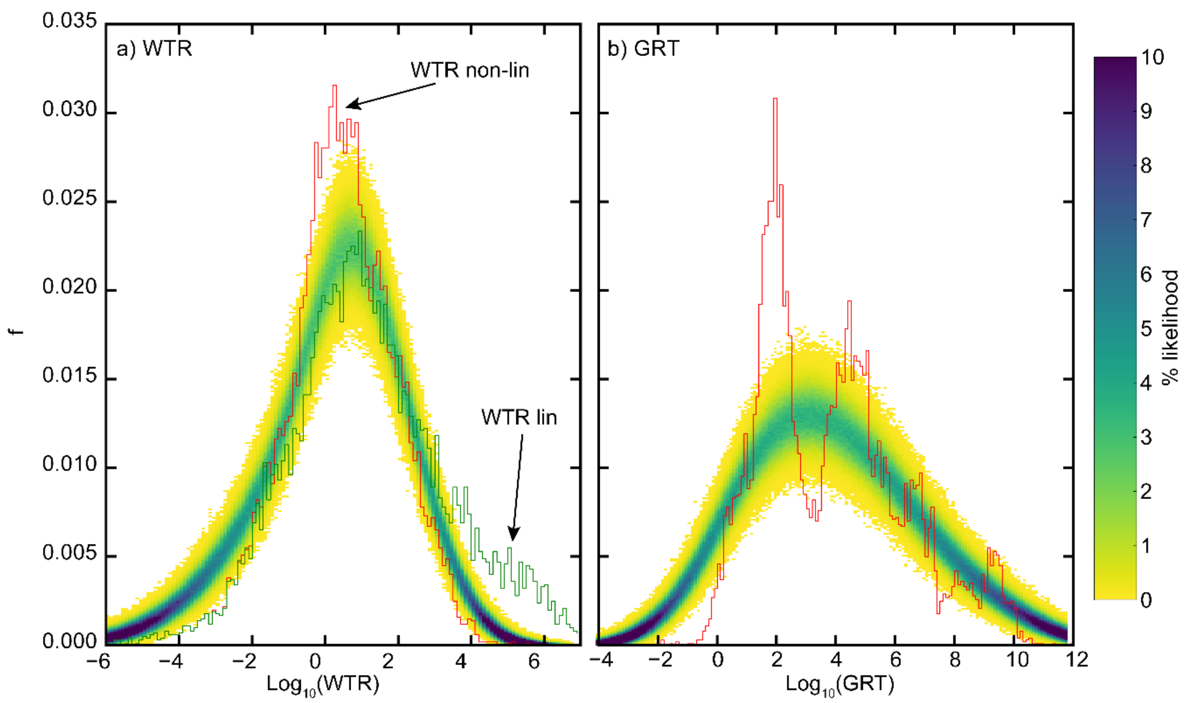

Figure S2. Global frequency distributions for baseline values of WTR (solid lines - linear WTR in green, non-linear WTR in red) and GRT (solid red line) based on 10,000 randomly distributed locations in comparison to results of 10,000 Monte Carlo Experiments (MCE) for both parameters. Each of the MCE realisations resulted in an individual frequency distribution curve which was then used to generate a heat map indicating the percentage likelihood, or intensity, of overlapping curves for each point in the parameter space. If the standard deviation in each parameter is progressively reduced to zero, the MCE distributions resolve on to the baseline frequency curves (not shown).

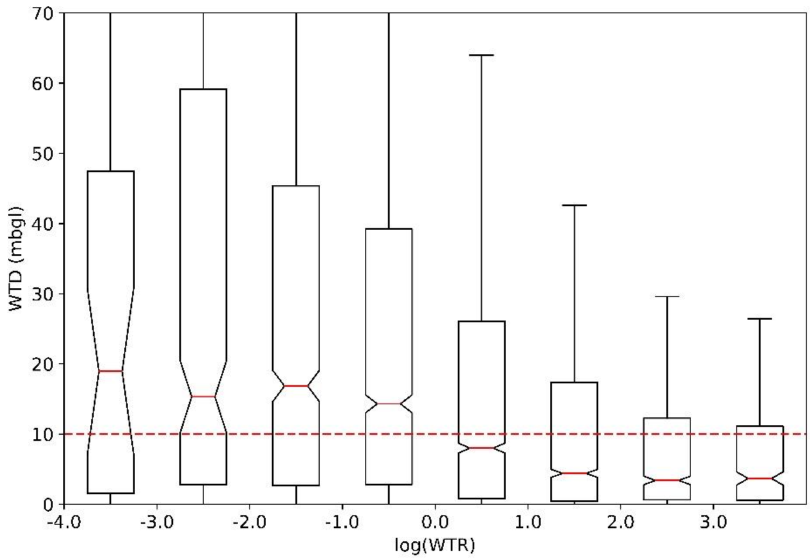

Figure S3. Box plot comparing water table depths (*WTDs*) globally derived from ref [3] to the water table ratio (*WTR*, non-linear version). Box plot notches indicate 45-55% percentiles, and box edges are defined by the 25% and 75% percentiles. The *WTR* shows a clear relationship with the distribution of water table depths indicating an approximate threshold of *WTR* = 1 (log(*WTR*)=0) for shallow water tables < 10 m bgl. Despite the large amount of scatter the agreement is reasonable given the very different data sets used in this study (lithological permeability maps) in comparison to ref [3] which modelled the groundwater levels using soil hydraulic properties. Considering only the global area with R>5 mm potential recharge[4], we find that areas with *WTDs*<10 m bgl cover 41-45% globally (depending on the recharge used [3]) compared to 46% (σ=0.3%) as defined here using the criterion *WTR*>1.

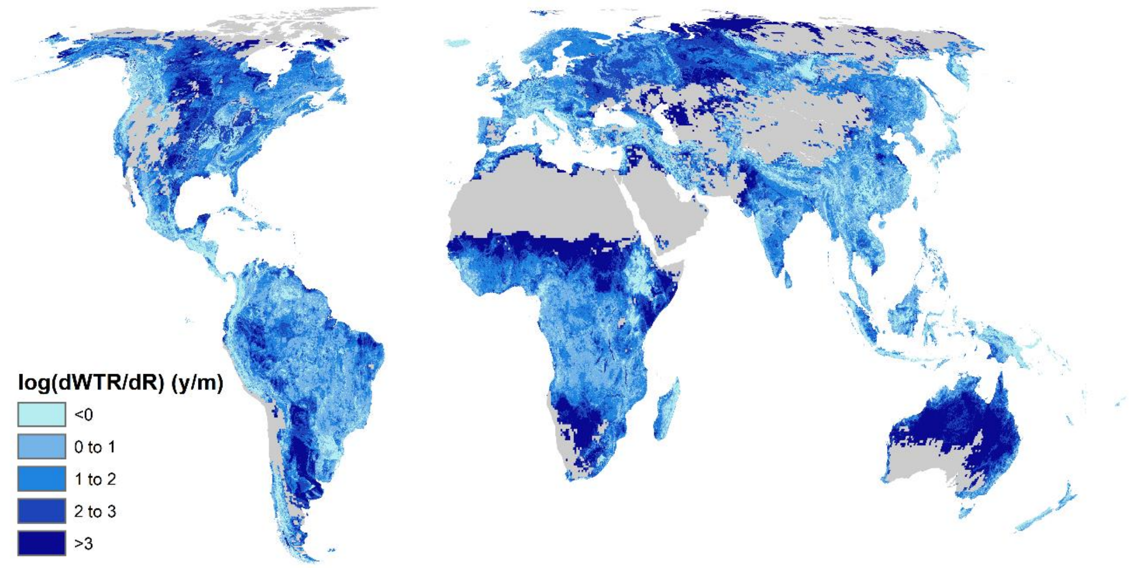

Figure S4. Global map of the derivative of water table ratio (*WTR*, non-linear) with respect to recharge (*R*) using Equation 10 (see main text).

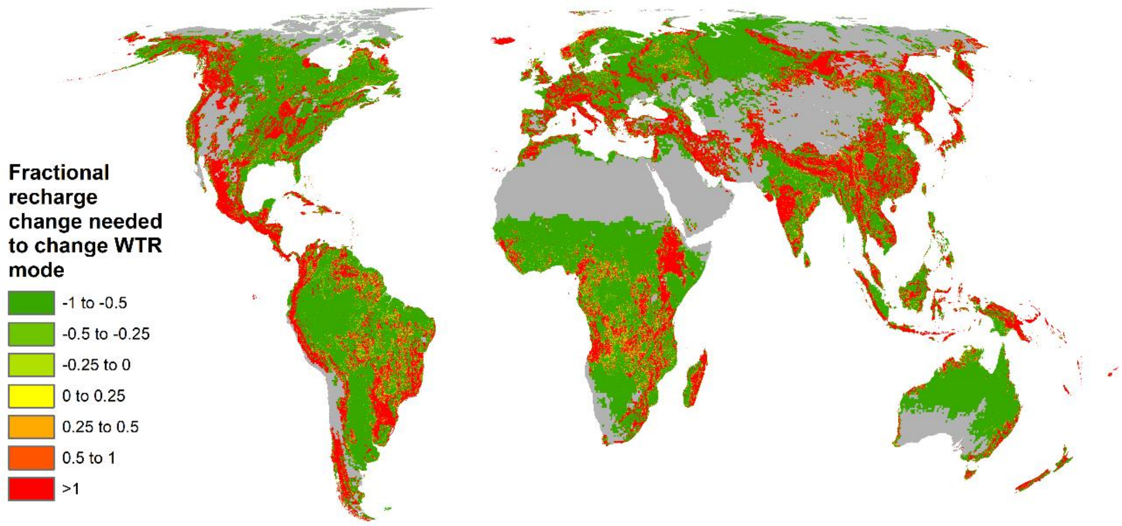

Figure S5. The fractional change in recharge needed to cause a change in mode of climate groundwater interactions from bi-directional (*WTR*>1) to uni-directional (*WTR*<1) or vice versa.

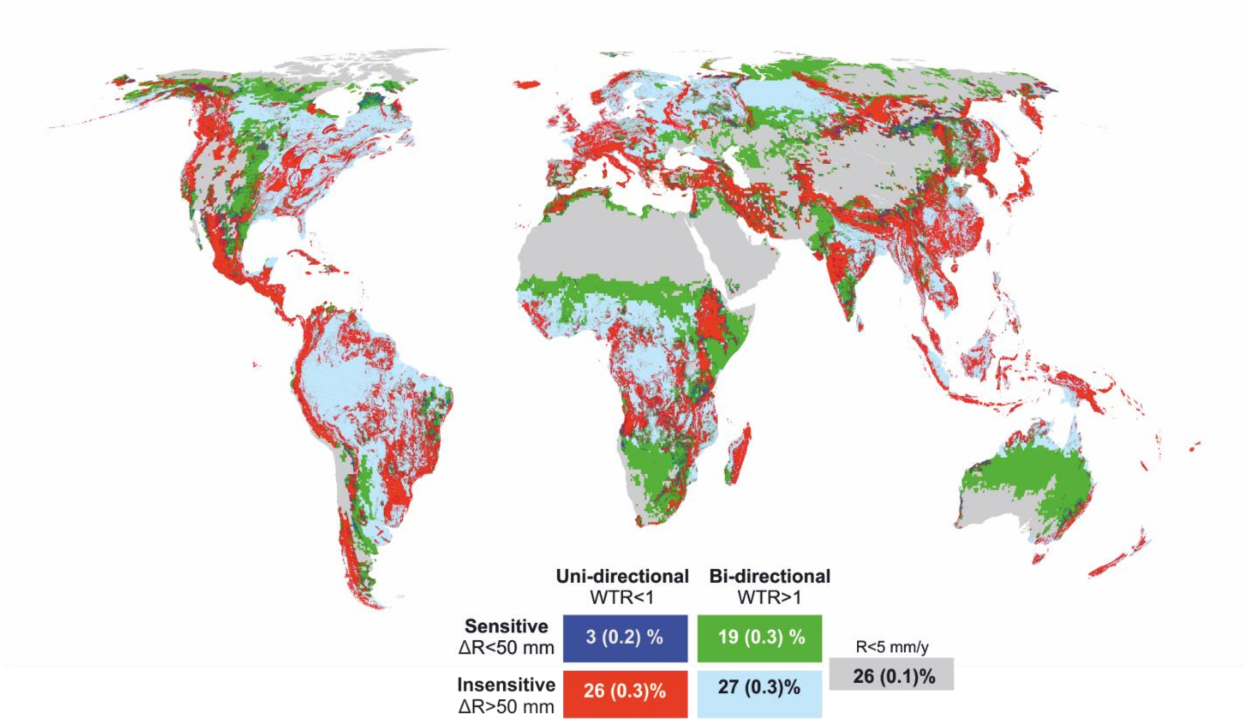

Figure S6. Global distributions of the temporal and spatial sensitivity in the mode of climate-groundwater interactions - as Figure 2b, but using an absolute change in recharge (Equation 12). Even given an unlimited amount of time, for an absolute change of 50 mm/y in recharge, only around 22% of the global area would change mode from bi-directional to uni-directional climate-groundwater interactions (as characterized by the threshold $WTR=1$) or vice versa. Mapped values use the baseline parameter set (see main text). The median percentage coverage of Earth's landmass for each category from the Monte Carlo experiments is labelled in the key with standard deviations shown in brackets. Grey areas represent contemporary recharge <5 mm/y [4].

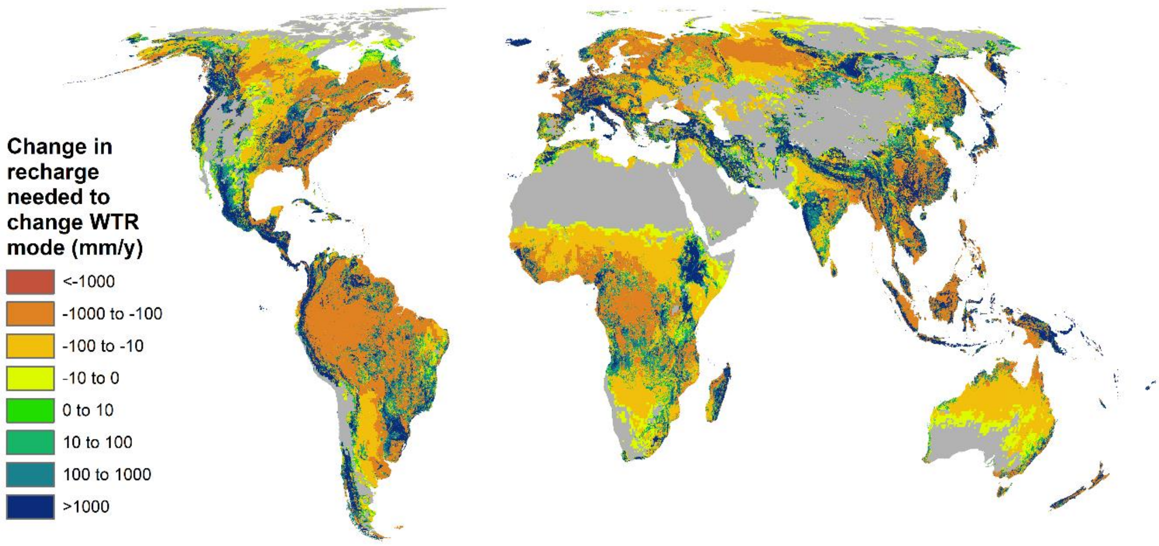

Figure S7. The change in recharge (mm/y) needed to cause a change in mode of climate groundwater interactions from bi-directional ($WTR>1$) to uni-directional ($WTR<1$) or vice versa.

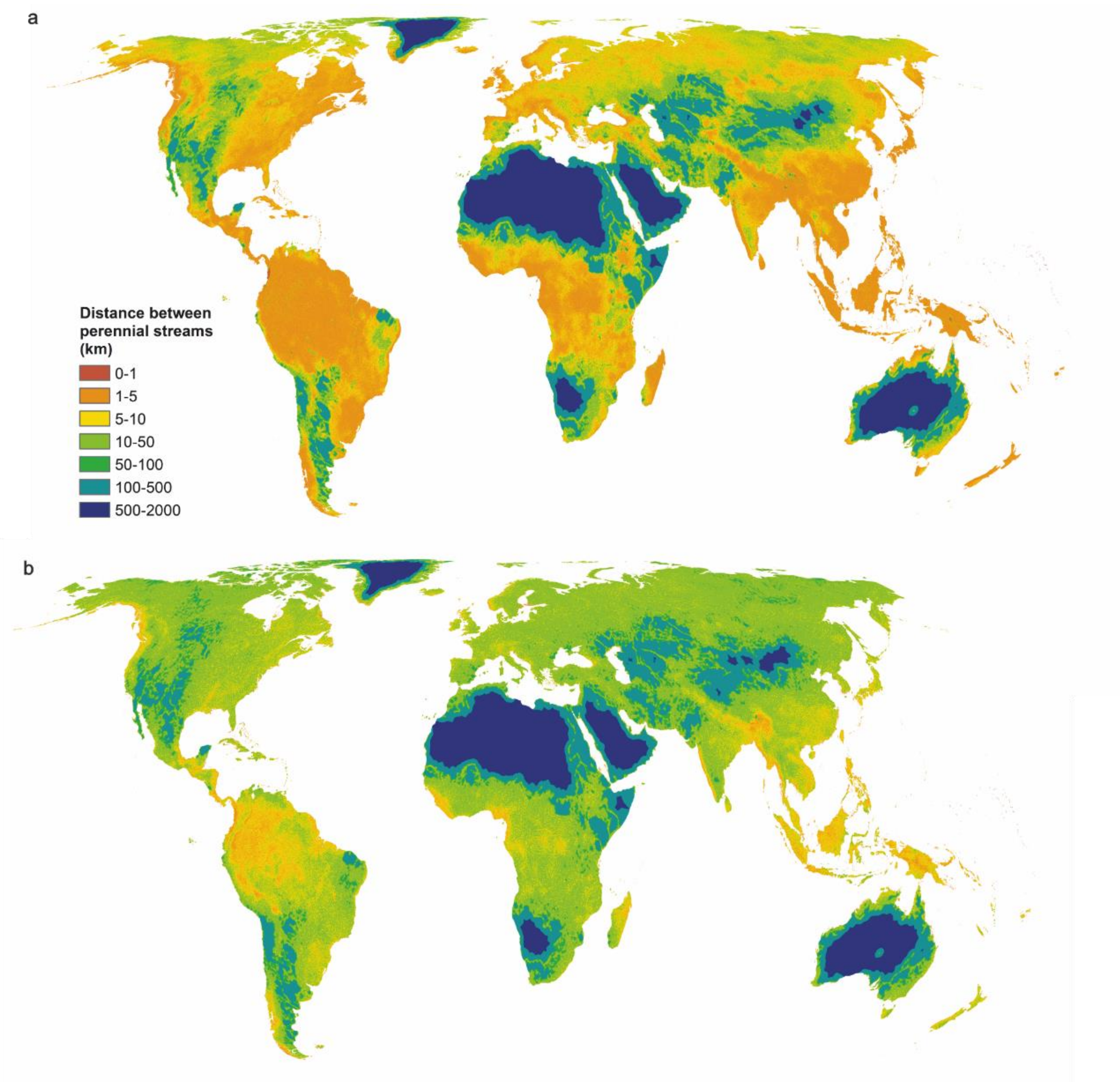

Figure S8. Distance between perennial streams (L, see Methods in main text) using discharge thresholds of **(a)** 0.1 m^3/s **(b)** 1 m^3/s. The difference in global mean and median distances between streams is around 16 km and 15 km shorter, respectively, for the lower discharge threshold.

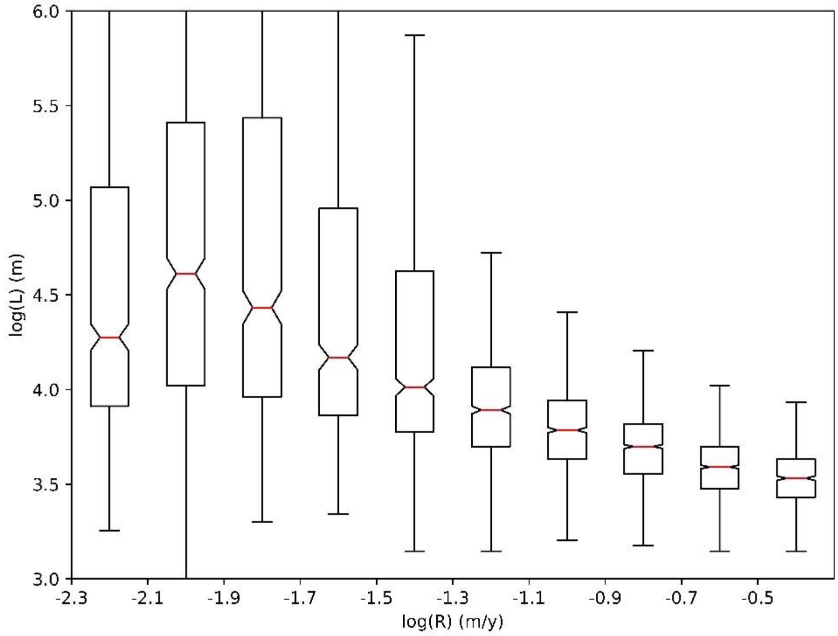

Figure S9. Global relationship between global groundwater recharge (*R*) from ref[4] and the distance between perennial streams (*L*). As recharge decreases, water tables disconnect increasingly from topography leading to larger distances between perennial streams. Because *R* is a weak control on the global distribution of the parameters (*d*, *K* or *S*) which are used to calculate *GRT* (Figure S10), the most important control on the relationship between *GRT* and *R* shown in Figure 3a is therefore via the distance between perennial streams (*L*).

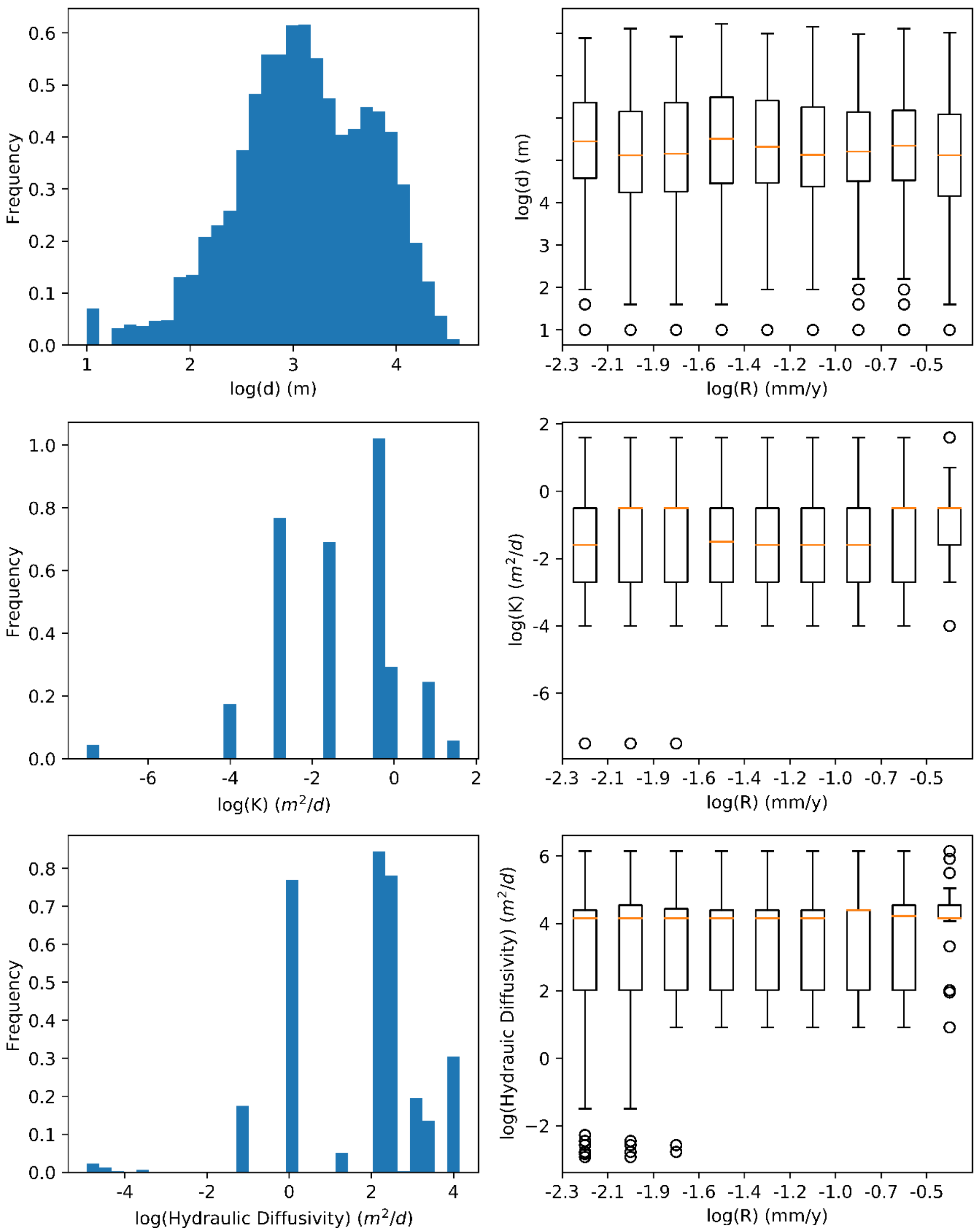

Figure S10. Global probability distributions of maximum terrain rise between rivers (*d*, m), hydraulic conductivity (*K*, m/d) and hydraulic diffusivity (*T*/*S*, m^2/d), and their relationships with groundwater recharge from ref[4]. Groundwater recharge is a weak control on the global distribution of the parameters (*d*, *K* or *S*) which are used to calculate *WTR* and *GRT*.

(a)

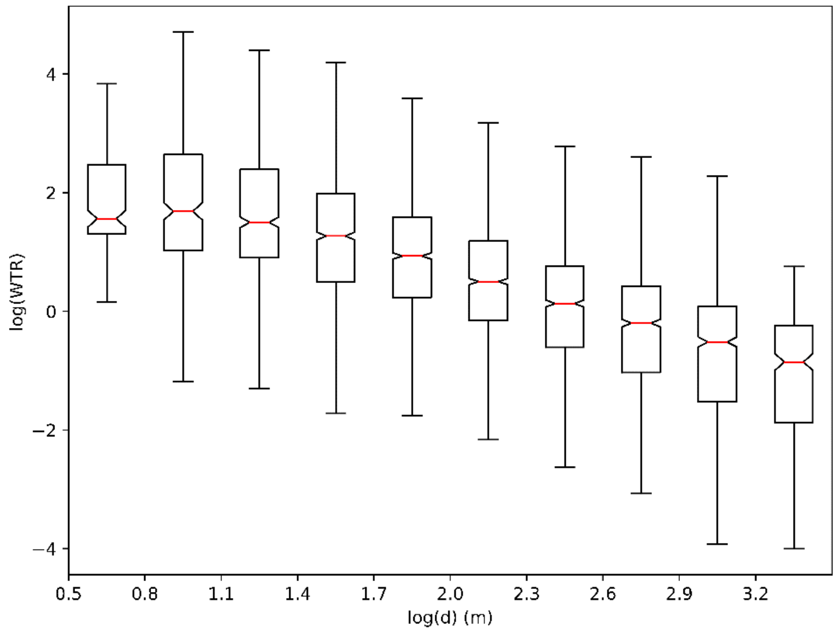

(b)

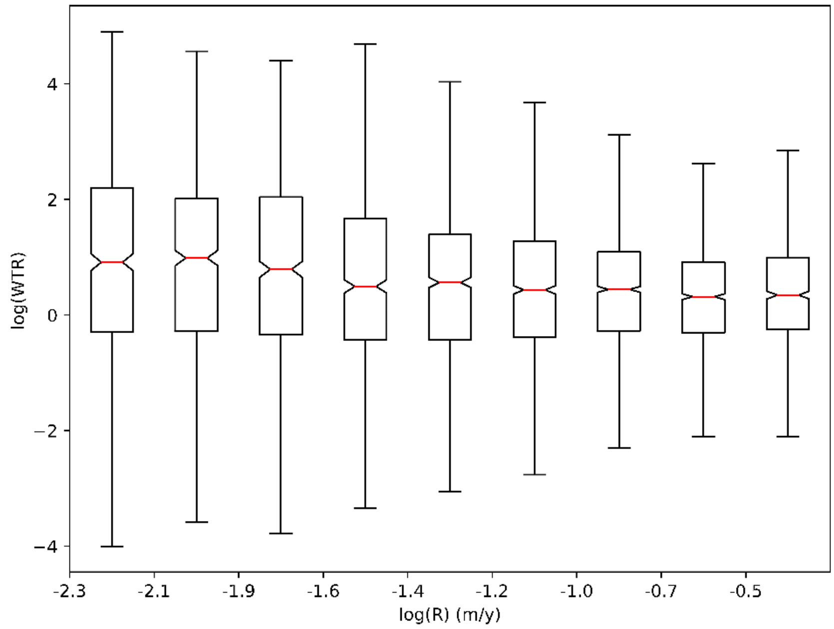

Figure S11. Global relationship between (a) maximum terrain rise (*d*) and (b) recharge from ref[4] with water table ratio (*WTR*). It might be expected that, given the nature of the *WTR* formulations (see Methods), higher recharge should lead to higher values of *WTR* and more strongly connected water tables. However, the relationship between *L* and *R* (Figure S9) tends to cancel out the dependency of *WTR* on these variables (*L* and *R*). Hence while a strong relationship is found between *d* and *WTR*, only a weak relationship is apparent between *WTR* and *R*. While increased recharge increases the proportion of the Earth's land surface across which bi-directional interaction between climate and groundwater can occur, the positive feedback created due to the shorter flow paths also enables regionally deeper water tables than might have been expected along with lower hydraulic response times.

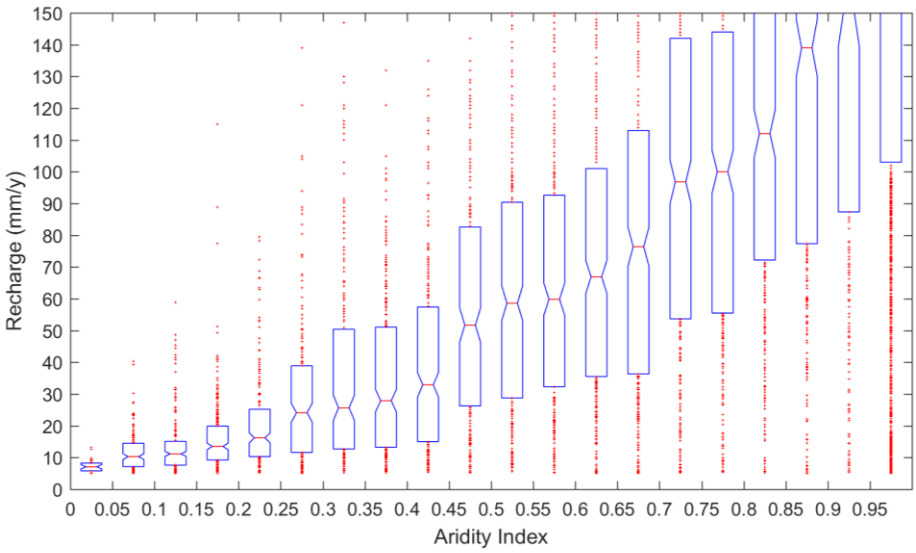

Figure S12. Global relationship between groundwater recharge from ref[4] and aridity index (long term average Precipitation/Potential Evapotranspiration) as defined by the CGIAR-CSI Global-Aridity and Global-PET Database (http://www.cgiar-csi.org/data/global-aridity-and-pet-database)[5,6].

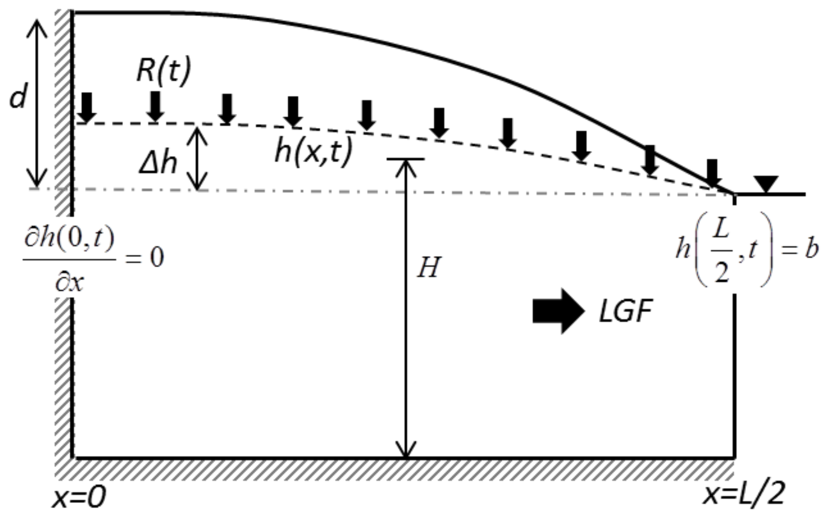

Figure S13 Geometry and boundary conditions for the idealized aquifer system used for equation derivations. The lateral groundwater flow (LGF) direction is also indicated.

References

1 Gleeson, T., Marklund, L., Smith, L. & Manning, A. H. Classifying the water table at regional to continental scales. *Geophysical Research Letters* **38** (2011).

2 Haitjema, H. M. & Mitchell-Bruker, S. Are water tables a subdued replica of the topography? *Groundwater* **43**, 781-786 (2005).

3 Fan, Y., Li, H. & Miguez-Macho, G. Global patterns of groundwater table depth. *Science* **339**, 940-943 (2013).

4 Döll, P. & Fiedler, K. Global-scale modeling of groundwater recharge. *Hydrology and Earth System Sciences* **12**, 863-885 (2008).

5 Zomer, R. J. *et al. Trees and water: smallholder agroforestry on irrigated lands in Northern India*. Vol. 122 (IWMI, 2007).

6 Zomer, R. J., Trabucco, A., Bossio, D. A. & Verchot, L. V. Climate change mitigation: A spatial analysis of global land suitability for clean development mechanism afforestation and reforestation. *Agriculture, ecosystems & environment* **126**, 67-80 (2008).